Dalton Transactions

Accepted Manuscript

This article can be cited before page numbers have been issued, to do this please use: M. V. Gradiski, B. T. H. Tsui, A. Lough and R. H. Morris, *Dalton Trans.*, 2019, DOI: 10.1039/C8DT04058C.

ROYAL SOCIETY OF CHEMISTRY

rsc.li/dalton

View Article Online
DOI: 10.1039/C8DT04058C

Journal Name

ARTICLE

PNN' & P_2NN' Ligands via Reductive Amination with Phosphine Aldehydes: Synthesis and Base-Metal Coordination Chemistry

Matthew V. Gradiski, Brian T. H. Tsui, Alan J. Lough, and Robert H. Morris*

Received 00th January 20xx,
Accepted 00th January 20xx

DOI: 10.1039/x0xx00000x

www.rsc.org/

Novel PNN' & P_2NN' ligands based on 2-aminopyridine (**APyPNN-R**) R = Ph (**1a**), Cy (**1b**), ^{i}Bu (**1c**), 8-aminoquinoline (**AQPNN-R**) R = Ph (**2a**), Cy (**2b**), ^{i}Bu (**2c**), ^{i}Pr (**2d**), and 2-picolylamine (**P_2NN-R**) R = Ph (**3a**), Cy (**3b**), ^{i}Bu (**3c**), have been synthesized via a versatile, one-pot, single-step, reductive amination of tertiary phosphine acetaldehydes with the amine by reaction with STAB (where STAB is sodium(triacetoxy)borohydride). Ligands **1b** and **1c** bridge between paramagnetic Co(II) and form dimeric complexes Co_2Cl_4(APyPNN-R)$_2$ (**4** and **5)** when reacted with cobalt dichloride. Ligands **2a-c** coordinate in a tridentate fashion forming chelate complexes MCl_2(AQPNN-R) M = Co(II) (**6-8**), and, for **2d**, the Fe(II) complex $FeCl_2$(AQPNN-^{i}Pr) (**9**). A solution magnetic susceptibility value for **9** of 3.9 μ_B is consistent with a monomer-dimer equilibrium. The synthesis of the dimeric complex [$FeCl_2$(AQPNN-Ph)]$_2$ (**10**) using **2a** as well as solid state magnetic susceptibility measurements on **9** and **10** confirm this phenomenon. Ligand **3a** coordinates to Fe(II) in an interesting tetradentate fashion despite bearing a tertiary amine moiety giving octahedral $FeCl_2$(P_2NN') (**11**). All of the metal complexes have been characterized by elemental analysis, paramagnetic ^{1}H NMR spectroscopy, solution magnetic susceptibility, and single crystal X-ray diffraction (XRD).

Introduction

A broadly successful strategy for the synthesis of base metal catalysts is the use of chelating ligands based on phosphorus and nitrogen. A preference for the use of base-metals such as iron, cobalt, and manganese has gathered momentum in recent years due to their cost-effectiveness and environmentally benign properties. The well-known PNP pincer framework has been used with cobalt,[1–6] manganese,[7–14] and iron[15–30] for a wide variety of different catalytic applications. Replacing a phosphorus donor with nitrogen to give PNN pincer ligands such as those reported by Milstein for water oxidation[31] have seen use with noble,[32–42] and base-metals.[43–46] Popular PNN ligand scaffolds used with iron are bipyridine-based,[45,47] however other scaffolds based on pyridine-pyrazole,[43,48,49] iminopyridine,[50] and picolylamine as well as 2-methanaminemethylimidazole[51] have been reported with iron and cobalt. The use of phosphonium dimers has been instrumental in the synthesis of iron complexes in our group.[24,25,30,52–62] Their air and moisture stability, ease of synthesis,[63] and handling make them an important class of reagents to perform metal-mediated template synthesis or reductive aminations. Typically, other syntheses of PNP and PNN ligands require multiple steps and the use of highly reactive, air-sensitive PR_2^- phosphides. In this study, we report the synthesis of novel PNN' and P_2NN' pincer ligands in a single step via reductive amination between *in situ* generated phosphine aldehydes and inexpensive commercially available primary amines. This synthetic method utilizes easy-to-handle reagents, and is a convenient alternative to conventional phosphide nucleophilic substitution that is typically encountered for the synthesis of this class of ligand. In the case of **2a-d**, these ligands have a preference to bind the metal centre in a *fac* geometry which although is known for some pincer type ligands, it is uncommon.[64] Their coordination chemistry with earth-abundant transition metals iron and cobalt is investigated.

Results and Discussion

Synthesis and Coordination Chemistry of Ligands 1 & 2

Adopting synthetic methodology from a study published recently in our group utilizing phosphonium dimers to synthesize a variety of chiral P–NH–P' ligands,[25] a reductive amination of α-phosphinoacetaldehydes with 2-aminopyridine was carried out leading to the synthesis of PNN' ligands **1a-c** in 40-45% yield (Eq 1, Scheme 1). The α-phosphinoacetaldehydes are generated *in-situ* upon deprotonation by two equivalents of base. The hydride of STAB acts as the base as confirmed by the observation of vigorous H_2 gas evolution. These ligands have been fully characterized by ^{1}H and ^{31}P NMR spectroscopy and mass spectrometry and, in the case of **1a**, single crystal X-ray diffraction (see experimental section and supporting information). In the synthesis of **1a** where the phosphine moiety contains aromatic substituents, an alcohol side product (approx. 50% of total) was characterized by ^{31}P NMR

Department of Chemistry, University of Toronto, 80 Saint George Street, Toronto, Ontario, M5S 3H6, Canada. Email: rmorris@chem.utoronto.ca
Electronic Supplementary Information (ESI) available: CCDC 1872334-1872342. For ESI and crystallographic data in CIF or other electronic format see DOI: 10.1039/x0xx00000x

spectroscopy (δ = -23.9 ppm) and mass spectrometry (m/z = 231[M+H]$^+$) to be 2-diphenylphosphinoethanol.

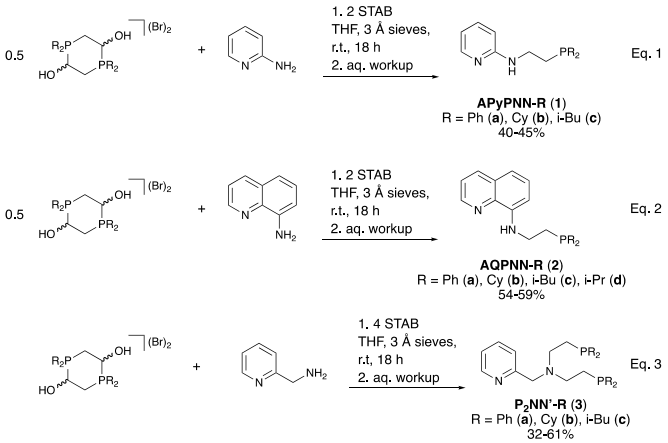

Scheme 1. Synthesis of PNN' & P_2NN' ligands via reductive amination.

Although STAB is known to be a relatively mild reducing agent and a popular choice for reductive amination reactions, the reagent is known to reduce aldehydes.[65] 2-aminopyridine acts as a poor nucleophile in this reductive amination owing to the nitrogen lone pair being in conjugation with the aromatic π system of the pyridine ring. The slow reactivity of this amine with respect to nucleophilic attack combined with an increased stability of the *in-situ* generated aromatic phosphine aldehyde as opposed to an alkyl phosphine aldehyde may lead to the reduction of the aldehyde to the corresponding phosphine alcohol. Conventional methods to try and remove the alcohol side product such as washing the residue with dilute KOtBu were unsuccessful. Due to the ligand being an air-stable solid as opposed to an oil as with **1b** and **1c**, the alcohol could be removed by crystallization of **1a** from a THF solution (Figure S46).

When reacted in slight excess with anhydrous cobalt dichloride in THF at room temperature, ligands **1b** and **1c** do not form a chelate with the metal but rather act as bridging ligands,

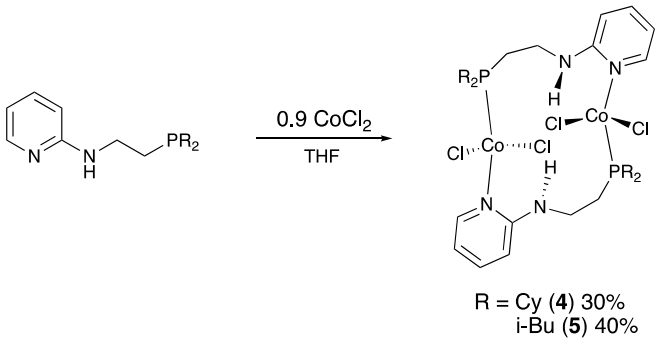

Scheme 2. Synthesis of cobalt dimers **4** and **5**

forming dimeric cobalt complexes **4** and **5** (Scheme 2). Single crystal XRD studies of **4** and **5** (Fig. 1) show that the cobalt(II) centres are crystallographically equivalent and distorted tetrahedral, with one tertiary phosphorus, one pyridyl and two chloride ligands. The aniline-like moieties are planar, resulting in an extended structure with large Co-Co distances of 7.2481(9) and 7.8882(8) Å for **4** and **5**, respectively. Both structures have NH..Cl hydrogen bonds with d(H..Cl) 2.54(4) Å for **4** and 2.52(5) for **5**. The inability of ligand **1** to chelate is likely due to the weakly basic nature of the aniline-like amino group and the unfavourable ring strain that would be present in a 4-membered Co-N-C-N ring. The only example reported in the Cambridge Structural Database (CSD) of a transition metal forming such a chelate is the octahedral nickel complex $[NiBr\{N(CH_2CH_2NHpy)_3\}]^+$ that has one chelated NHpy group with an N-Ni-N bite angle of 63.3°.[66] Only two other dimeric structures $Co_2(\mu\text{-}PN)_2Cl_2$ with phosphino-oxazoline ligands have been reported; however the Co-Co distances were shorter (5.81, 6.02 Å) and monomeric complexes could be isolated by increasing the steric bulk α to the nitrogen atom in the oxazoline ring.[67]

Fig. 1. X-ray structures of **4** (top) and **5** (bottom). Ellipsoids are shown at 50% probability. Carbon-bound hydrogen atoms have been omitted for clarity. Selected bond lengths (Å) and angles (deg) for **4**: Co(1)–N(1) 2.056(3), Co(1)–Cl(1) 2.2252(11), Co(1)–Cl(2) 2.2573(11), Co(1)–P(1) 2.3764(10), N(1)–Co(1)–Cl(1) 109.19(9), N(1)–Co(1)–Cl(2) 109.65(9), Cl(1)–Co(1)–Cl(2) 115.31(5), N(1)–Co(1)–P(1) 106.04(9), Cl(1)–Co(1)–P(1) 108.19(4), Cl(2)–Co(1)–P(1) 108.03(4); for **5**: Co(1)–N(1) 2.057(3), Co(1)–Cl(1) 2.2348(9), Co(1)–Cl(2) 2.2573(9), Co(1)–P(1) 2.3846(9), N(1)–Co(1)–Cl(1) 105.13(8), N(1)–Co(1)–Cl(2) 110.69(8), Cl(1)–Co(1)–Cl(2) 111.57(4), N(1)–Co(1)–P(1) 106.52(8), Cl(1)–Co(1)–P(1) 121.05(4), Cl(2)–Co(1)–P(1) 101.72(4).

Taking into consideration the unfavourable formation of a 4-membered ring about the metal centre, ligands **2a-d** were

designed to prevent the dimerization observed with **1b** and **1c**. Following the same reaction procedure as in the synthesis of **1a-c**, reductive amination of the α-phosphinoacetaldehydes with 8-aminoquinoline proceeds very rapidly as judged by the appearance of a deep red colour (Eq 2, Scheme 1). In all cases, the reaction appeared to be complete after 90 minutes, however stirring was continued overnight as a precaution. The synthesis of **2a** was also conducted using "wet" benchtop solvent, and the workup was done without using air-free Schlenk techniques. This did not have any detrimental impact on the yield or purity of the final product. No reactions in air were attempted for non-aromatic phosphines and ligand **2a** that was used for the synthesis of **6** was made air-free.

The ^{1}H and ^{13}C NMR of **2c** and **2d** are particularly interesting as chemical inequivalence is observed for the terminal methyl groups of the P^{i}Bu$_2$ and P^{i}Pr$_2$ moieties (see SI for full spectra). In the ^{1}H NMR of **2c** the methyl groups are observed as two distinct doublets and for **2d**, the methyl groups are observed as two distinct overlapping doublets of doublets. Similarly, in the ^{13}C NMR an extra doublet is observed in the aliphatic region. This has also been observed in a related PNP ligand in which P^{i}Pr$_2$ methyl groups were observed by ^{1}H and ^{13}C NMR to display chemical inequivalence.[68] The diastereotopic nature of the methyl groups arise from the pyramidal geometry about the phosphorous atom. Diastereotopic methyl groups were also found to be present in **1c**. When R = Ph or Cy as in **2a**/**2b** and **1a**/**1b**, diastereotopic CH or CH$_2$ protons were not observed due to a large number of overlapping signals.

Compounds **2a-d** were reacted with an equimolar amount of anhydrous MCl$_2$ (M = Co, Fe) to afford the corresponding 5-coordinate pincer complexes **6-9** (Scheme 3).

The two 5-membered rings formed about the metal centre, as confirmed by single crystal XRD (Fig. 2-4), promote the formation of a mononuclear chelate complex as opposed to the bridged binuclear complexes observed with ligands **1b** and **1c**. Complexes **6**-**9** adopt a distorted trigonal bipyramidal (TBP) geometry with the NH and a Cl in the axial positions and the imine, phosphorus, and chloride ligands in the equatorial Complexes **6-8** have solution magnetic susceptibilities of μ_{eff} = 3.9, 4.2, and 4.2 μ_B respectively. These values are consistent with a high-spin (HS) 5-coordinate cobalt(II) centre with 3 unpaired electrons. In the sold state, **8** crystallizes as a 1:1 mixture of enantiomers (Fig. 3) that are assigned (*R*)/(*S*)-

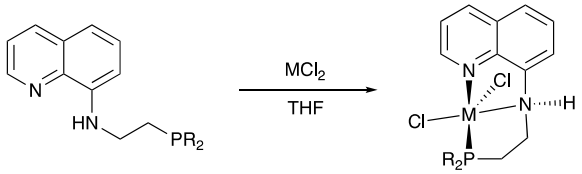

M = Co, R = Ph (**6**) 91%
M = Co, R = Cy (**7**) 81%
M = Co, R = i-Bu (**8**) 75%
M = Fe, R = i-Pr (**9**) 87%

Scheme 3. Synthesis of **6-9**.

A similar phenomenon was observed by our group with *cis*-β iron(II) complexes that exist in the solid state as 1:1 mixtures of diastereomers.[56] Unfortunately, due to the paramagnetic nature of these metal complexes, the use of ^{1}H or ^{31}P NMR is futile for determining the ratio of the diastereomers in solution (see SI for paramagnetic ^{1}H NMR spectra). The presence of both diastereomers in the solid state is possibly due to the steric bulk of the phosphine moiety being located further away from the metal centre. Isobutyl substituents are more flexible than isopropyl and cyclohexyl substituents respectively in addition to the bulky CH(CH$_3$)$_2$ fragments being located β to the phosphorus atom as opposed to α for isopropyl and α for the CH(CH$_2$)$_2$ fragments in cyclohexyl. position. Related dichloride cobalt(II) complexes bearing picolyl-based PNN ligands have been reported and are useful for the transfer hydrogenation of nitriles[51] and isomerization of olefins.[69]

View Article Online
DOI: 10.1039/C8DT04058C

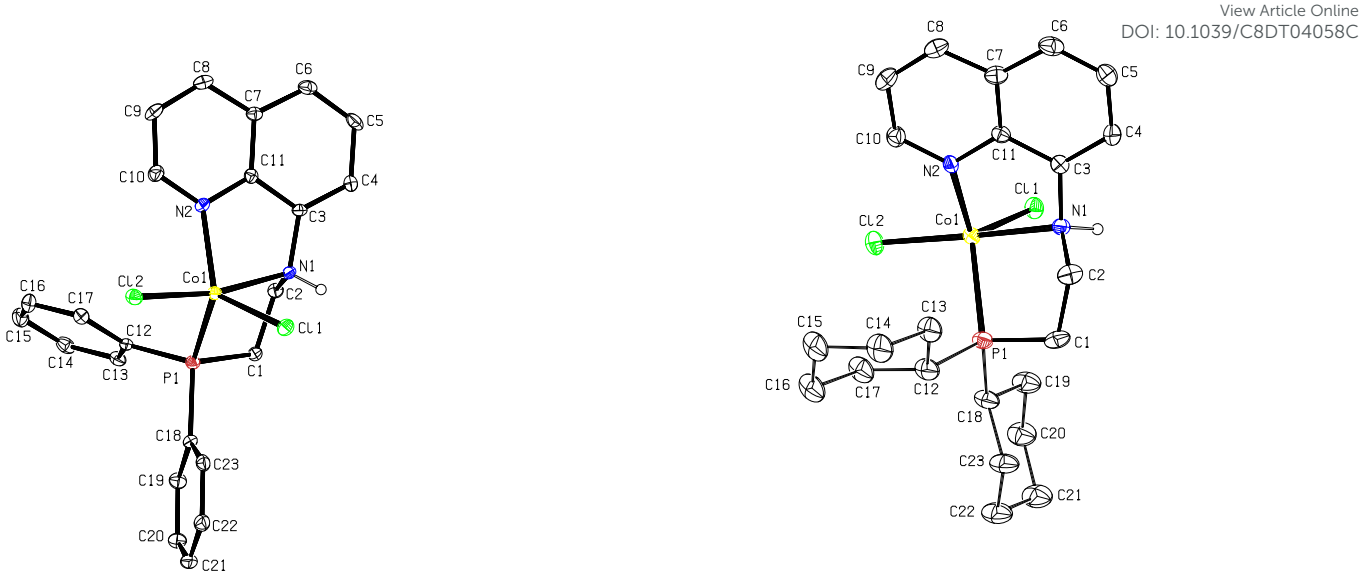

Fig. 2. X-ray structures of **6** (left) and **7** (right). Ellipsoids are shown at 50% probability. Carbon-bound hydrogen atoms have been omitted for clarity. Selected bond lengths (Å) and angles (deg) for **6**: Co(1)–N(2) 2.098(2), Co(1)–N(1) 2.285(3), Co(1)–Cl(1) 2.3087(8), Co(1)–Cl(2) 2.3283(9), Co(1)–P(1) 2.4013(8), N(2)–Co(1)–N(1) 74.94(9), N(2)–Co(1)–Cl(1) 125.15(7), N(1)–Co(1)–Cl(1) 87.08(7), N(2)–Co(1)–Cl(2) 95.07(7), N(1)–Co(1)–Cl(2) 170.00(7), Cl(1)–Co(1)–Cl(2) 98.68(3), N(2)–Co(1)–P(1) 114.69(7), N(1)–Co(1)–P(1) 79.85(6), Cl(1)–Co(1)–P(1) 112.20(3), Cl(2)–Co(1)–P(1) 105.21(3); for **7:** Co(1)–N(2) 2.078(4), Co(1)–N(1) 2.277(4), Co(1)–Cl(1) 2.2988(14), Co(1)–Cl(2) 2.3232(14), Co(1)–P(1) 2.3812(15), N(2)–Co(1)–N(1) 77.09(16), N(2)–Co(1)–Cl(1) 115.14(12), N(1)–Co(1)–Cl(1) 84.11(11), N(2)–Co(1)–Cl(2) 98.06(12), N(1)–Co(1)–Cl(2) 174.04(12), Cl(1)–Co(1)–Cl(2) 101.21(6), N(2)–Co(1)–P(1) 120.05(13), N(1)–Co(1)–P(1) 79.56(11), Cl(1)–Co(1)–P(1) 116.26(6), Cl(2)–Co(1)–P(1) 100.22(6);

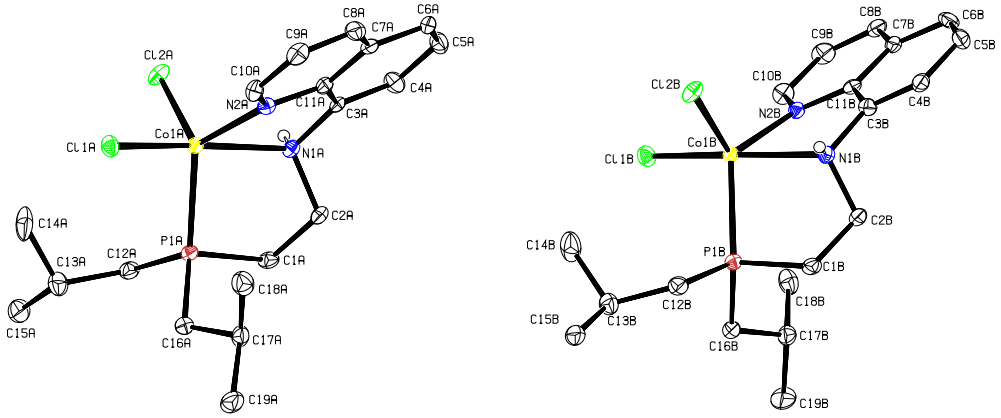

Fig. 3. X-ray structures of **8** depicting the two configurations (*R*)-NH (left) and (*S*)-NH (right). Ellipsoids are shown at 50% probability. Carbon-bound hydrogen atoms have been omitted for clarity. Selected bond lengths (Å) and angles (deg) for **(*R*)-NH**: Co(1A)–N(2A) 2.108(4), Co(1A)–N(1A) 2.260(5), Co(1A)–Cl(1A) 2.3032(16), Co(1A)–Cl(2A) 2.3243(16), Co(1A)–P(1A) 2.4108(14), N(2A)–Co(1A)–N(1A) 75.59(16), N(2A)–Co(1A)–Cl(1A) 95.54(13), N(1A)–Co(1A)–Cl(1A) 169.17(12), N(2A)–Co(1A)–Cl(2A) 114.50(13), N(1A)–Co(1A)–Cl(2A) 85.79(13), Cl(1A)–Co(1A)–Cl(2A) 103.77(6), N(2A)–Co(1A)–P(1A) 128.78(13), N(1A)–Co(1A)–P(1A) 79.47(11), Cl(1A)–Co(1A)–P(1A) 102.07(5), Cl(2A)–Co(1A)–P(1A) 107.32(5); for **(*S*)-NH**: Co(1B)–N(2B) 2.111(4), Co(1B)–N(1B) 2.279(5), Co(1B)–Cl(1B) 2.2941(16), Co(1B)–Cl(2B) 2.3265(16), Co(1B)–P(1B) 2.4106(14), N(2B)–Co(1B)–N(1B) 75.46(16), N(2B)–Co(1B)–Cl(1B) 95.22(13), N(1B)–Co(1B)–Cl(1B) 169.19(12), N(2B)–Co(1B)–Cl(2B) 115.10(13), N(1B)–Co(1B)–Cl(2B) 85.62(13), Cl(1B)–Co(1B)–Cl(2B) 103.55(7), N(2B)–Co(1B)–P(1B) 127.77(13), N(1B)–Co(1B)–P(1B) 79.44(11), Cl(1B)–Co(1B)–P(1B) 102.76(5), Cl(2B)–Co(1B)–P(1B) 107.63(5).

View Article Online
DOI: 10.1039/C8DT04058C

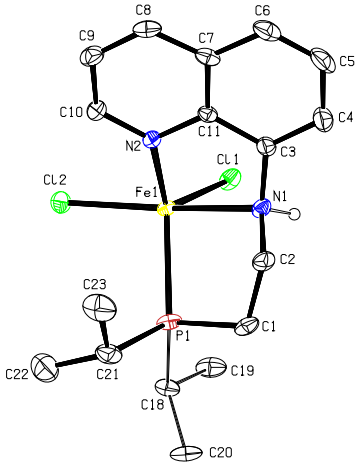

Fig. 4. X-ray structures of **9**. Ellipsoids are shown at 50% probability. Carbon-bound hydrogen atoms have been omitted for clarity. Selected bond lengths (Å) and angles (deg): Fe(1)–N(2) 2.1626(15), Fe(1)–N(1) 2.2942(16), Fe(1)–Cl(2) 2.3205(5), Fe(1)–Cl(1) 2.3359(5), Fe(1)–P(1) 2.4462(5), N(2)–Fe(1)–N(1) 74.53(6), N(2)–Fe(1)–Cl(2) 94.79(4), N(1)–Fe(1)–Cl(2) 167.97(5), N(2)–Fe(1)–Cl(1) 119.57(4), N(1)–Fe(1)–Cl(1) 86.01(4), Cl(2)–Fe(1)–Cl(1) 104.39(2), N(2)–Fe(1)–P(1) 115.22(4), N(1)–Fe(1)–P(1) 80.49(4), Cl(2)–Fe(1)–P(1) 99.63(2), Cl(1)–Fe(1)–P(1) 116.94(2).

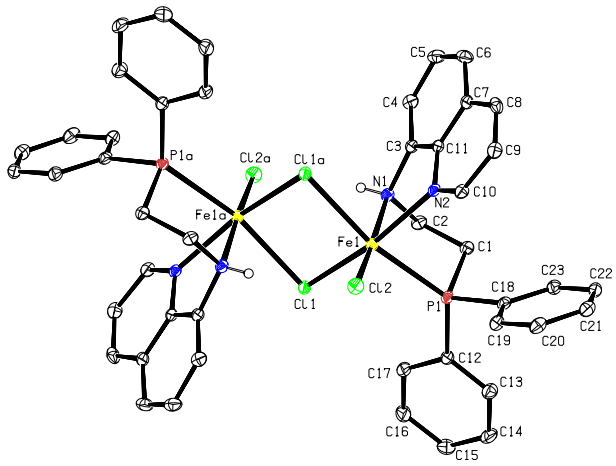

Fig. 5. X-ray structure of **10**. Ellipsoids are shown at 50% probability. Carbon-bound hydrogen atoms have been omitted for clarity. Selected bond lengths (Å) and angles (deg): Fe(1)-N(2) 2.211(2), Fe(1)-N(1) 2.259(2), Fe(1)-Cl(2) 2.3455(7), Fe(1)-Cl(1) 2.4872(7), Fe(1)-P(1) 2.5485(7), N(2)–Fe(1)–P(1) 84.08(5), N(1)–Fe(1)–P(1) 81.60(6), Cl(2)–Fe(1)–P(1) 103.09(3), Cl(1)–Fe(1)–P(1) 94.29(2)..

8 is also much more distorted from ideal TBP geometry with a τ_5 value[70] of 0.67 whereas **6, 7** and **9** experience less distortion and have τ_5 values of 0.75, 0.90, and 0.81 respectively.

Solution magnetic susceptibility measurements of **9** did not give a μ_{eff} value consistent with what would be expected for HS 5-coordinate iron(II). A value of μ_{eff} = 3.9 μ_B was measured. We believe that in solution, an equilibrium between monomeric **9** and a dimeric complex exists that heavily favours the dimeric form. A dimeric complex will experience some degree of antiferromagnetic coupling between the two metal centres and therefore have a lower effective magnetic moment per metal centre than its corresponding monomer. Evidence for the existence of a potential dimeric form of **9** was obtained when ligand **2a** is reacted with an equivalent of $FeCl_2$ to give dimeric complex **10** (Scheme 4).

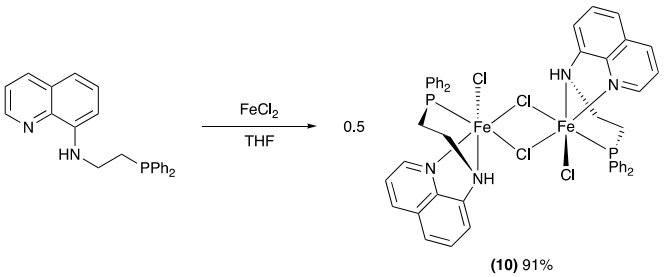

Scheme 4. Synthesis of dimeric complex **10**.

Complex **10** exists exclusively as a dimer in the solid and solution state and has been characterized by elemental analysis, paramagnetic ^{1}H NMR, and single crystal XRD (Fig. 5). The low solubility of **10** in common NMR solvents did not allow an accurate solution magnetic susceptibility value to be measured. In order to further investigate the proposed dimeric complex formation in solution for **9**, the solid state magnetic susceptibility of **9** and **10** were measured. Variable temperature SQUID measurements from 5-300 K in a constant magnetic field of 1000 Oe (0.1 T) gave a calculated μ_{eff} value of 5.2 μ_B for **9** and 7.4 μ_B for **10** with an average μ_{eff} of 3.7 μ_B per iron centre. This value for **9** is in agreement with a 5-coordinate HS iron(II) centre with 4 unpaired electrons. The value of 7.4 μ_B for **10** is consistent with other chloride-bridged dinuclear iron(II) complexes with multiple nitrogen donors.[71,72] A solid state magnetic moment measurement of 5.2 μ_B for **9** indicates that in solution, a monomeric structure is not retained. A potential dimeric species can be observed when the ^{1}H NMR spectra of **9** and **10** are compared (Fig. S45). Complexes **9** and **10** share two common peaks in their ^{1}H NMR at ~43 and 30 ppm. These peaks can be assigned as part of the aminoquinoline ligand in a dimeric compound as it is the only common functionality between **9** and **10** apart from the ethylene linker. Additionally, at reduced concentration, less dimer is expected to be present in solution. When the ^{1}H NMR is measured for **9** at half concentration (Fig. S45-**III**) the resonance at 43 ppm assigned to a dimeric complex reduces in intensity and the resonance at 24 ppm experiences a 1 ppm shift approximately to 23 ppm. These changes are attributed to a small drop in concentration of the dimeric species.

Synthesis and Coordination Chemistry of Ligand 3

If reductive amination is carried out with a primary amine substrate that lacks substitution α to nitrogen, the tertiary amine is preferentially produced. Performing reductive amination with 2-picolylamine affords the tripodal ligands **3a-c** (Eq 3, Scheme 1). Using the same 2:1 molar equivalent of

phosphonium dimer to amine as in the synthesis of **1** and **2** results in the formation of a minor amount of mono-alkylated product, as observed by ^{31}P NMR and mass spectrometry. Attempts to isolate the mono-alkylated product were carried out through N-atom protection using BOC (*tert*-butyloxycarbonyl) and tosyl (*p*-toluenesulfonyl) groups; however, this rendered the amine too weakly nucleophilic to participate in the reaction. Recovery of the N-protected starting material and reduction of the phosphine aldehyde to the phosphino alcohol were observed. Altering the stoichiometry to a 1:1 ratio of phosphonium dimer and amine affords the di-alkylated compound as the only product. Iron(II) was selected as the metal of choice to coordinate this ligand due to the favourable formation of a d^6 octahedral 18-electron complex as opposed to a 19-electron complex with cobalt(II). Reaction with $[Co(NH_3)_5Cl]Cl_2$ was attempted; however the insolubility of the salt in organic solvents left coordination to cobalt(III) unsuccessful. When reacted with an equivalent of $FeCl_2$ in THF (Scheme 5), **3a** coordinates in a tetradentate fashion forming a pseudo-octahedral complex **11**.

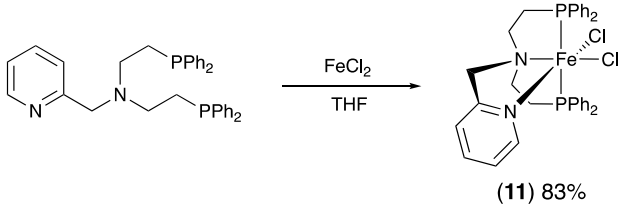

Scheme 5. Synthesis of **11**.

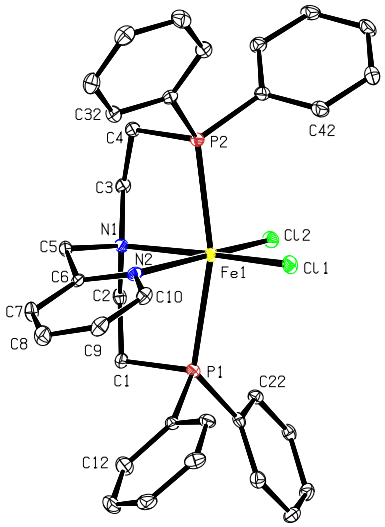

Fig. 6. X-ray structure of **11**. Ellipsoids are shown at 50% probability. Hydrogen atoms have been omitted for clarity. Selected bond lengths (Å) and angles (deg): Fe(1)–N(2) 2.229(2), Fe(1)–N(1) 2.325(2), Fe(1)–Cl(1) 2.3307(8), Fe(1)–Cl(2) 2.4470(8), Fe(1)–P(2) 2.5079(9), Fe(1)–P(1) 2.6110(9), N(2)–Fe(1)–N(1) 75.36(8), N(2)–Fe(1)–Cl(1) 95.37(6), N(1)–Fe(1)–Cl(1) 170.64(6), N(2)–Fe(1)–Cl(2) 162.97(6), N(1)–Fe(1)–Cl(2) 88.34(6), Cl(1)–Fe(1)–Cl(2) 101.01(3), N(2)–Fe(1)–P(2) 94.56(6), N(1)–Fe(1)–P(2) 80.32(6), Cl(1)–Fe(1)–P(2) 99.33(3), Cl(2)–Fe(1)–P(2) 87.40(3), N(2)–Fe(1)–P(1) 81.84(6), N(1)–Fe(1)–P(1) 80.29(6), Cl(1)–Fe(1)–P(1) 100.01(3), Cl(2)–Fe(1)–P(1) 90.69(3), P(2)–Fe(1)–P(1) 160.57(3).

View Article Online
DOI: 10.1039/C8DT04058C

The phosphines coordinate *trans* as confirmed by single crystal XRD (Fig. 6) having a P–Fe–P bond angle of 160.57(3) °. Complex **11** exists as a paramagnetic compound and as such is ^{31}P NMR silent. To our knowledge, complex **11** is only the second reported iron(II) complex bearing two phosphine, two nitrogen, and two chloride ligands and the first utilizing a tetradentate ligand framework. The first, reported by Kirchner et. al.[73] was found to be a spin crossover complex. A preliminary magnetochemistry investigation of **11** did not provide evidence for similar spin crossover properties.

Conclusions

A variety of novel PNN' & P_2NN' ligands **1-3** have been synthesized via a one-pot reductive amination with phosphine aldehydes. This one step reaction with minimal product purification allows a convenient access to useful multidentate phosphorous-nitrogen ligands. Compounds **1** behave as bridging ligands between two metal centres and form dimeric cobalt complexes **4** and **5**. Compounds **2** coordinate iron and cobalt dichloride as tridentate ligands forming 5-coordinate paramagnetic mononuclear complexes **6- 9**. The cobalt complex **8** exists in the solid state as a 1:1 mixture of enantiomers with chirality at nitrogen. Compound **3a** coordinates iron dichloride as a tetradentate ligand giving rise to 6-coordinate complex **11**. Complexes **4-11** have been crystallographically characterized. The use of **4-11** in catalytic applications is currently under investigation.

Experimental Section

General Considerations

All experimental procedures and manipulations were conducted under a dinitrogen or argon atmosphere using standard Schlenk-line and glove box procedures unless otherwise stated. All solvents were degassed and dried using standard procedures prior to all procedures. Washing solutions were degassed prior to use. 2-aminopyridine, and 2-picolylamine were purchased from Sigma Aldrich and used without further purifications. 8-aminoquinoline was purchased from Alfa Aesar and used without further purification. Phosphonium dimers were synthesized according to literature procedures[63,59] or received from Digital Specialty Chemicals. All other reagents were purchased from commercial sources and used without further purification. NMR spectra were recorded at ambient temperature and pressure using an Agilent 500 MHz spectrometer with a OneNMR H/F{X} Probe (500 MHz for ^{1}H, 126 MHz for ^{13}C, 202 MHz for ^{31}P, and 160 MHz for ^{11}B), or an Agilent DD2-600 MHz spectrometer (600 MHz for ^{1}H, 151 MHz for ^{13}C, and 242 MHz for ^{31}P) unless stated otherwise. The ^{1}H and ^{13}C NMR were measured relative to partially deuterated solvent peaks. ^{31}P chemical shifts were measured relative to 85% phosphoric acid as an external reference. ^{11}B chemical

shifts were measured relative to $BF_3{\cdot}Et_2O$ as an external reference. NMR assignments were made based on ^{1}H–COSY, and ^{1}H–^{13}C-HSQC NMR spectroscopy. The elemental analyses were performed on a Perkin-Elmer 2400 CHN elemental analyser. Solution magnetic susceptibilities were measured at 25 °C by a method originally described by Evans. A solution of the compound in $CDCl_3$/cyclohexane (95/5 v/v) was prepared. The external standard consisted of a flame-sealed capillary containing $CDCl_3$/cyclohexane (95/5 v/v). The chemical shift difference of cyclohexane between the inset and the solution was used to determine the magnetic moment μ_{eff}. All measurements were run in duplicate at minimum.

***N*-(2-(diphenylphosphinyl)ethyl)pyridin-2-amine (1a)**

A vial was charged with 2-aminopyridine (94 mg, 1.0 mmol), phenyl-substituted phosphonium dimer (309 mg, 0.5 mmol), and sodium(triacetoxy)borohydride (424 mg, 2.0 mmol). THF (6 mL) was added and the mixture was stirred over 3 Å MS for 18 hours. The solvent was removed in vacuo and the residue was dissolved in DCM (10 mL) and transferred to a 25 mL Schlenk flask. On the Schlenk line under argon, an air-free wash with saturated, degassed NH_4Cl (2x10 mL), and degassed H_2O (2x10 mL) was conducted. The solution was dried over $MgSO_4$, filtered, and passed through a short neutral alumina plug. The solvent was removed to give a white solid that was recrystallized by slow evaporation of a THF/pentane mixture (125 mg, 41%). ^{31}P{^{1}H} NMR (202 MHz, $CDCl_3$) δ: -21.38 ppm. ^{1}H NMR (500 MHz $CDCl_3$) δ: 2.39-2.42, m, 2H, (CH_2), 3.42-3.48, m, 2H, (CH_2), 4.62, s(br), 1H, (N*H*), 6.23-6.25, d (*J* = 8.4 Hz), 1H, (Py-*H*), 6.53-6.56, m, 1H, (Py-*H*), 7.32-7.47, m, 11H, (P*Ph*$_2$, Py-*H*), 8.06-8.08, m, 1H, (Py-*H*). MS-DART m/z calculated for $[C_{19}H_{20}N_2P]^+$: 307.1359, found: 307.1358.

***N*-(2-(dicyclohexylphosphinyl)ethyl)pyridin-2-amine (1b)**

The same general procedure was followed as in the synthesis of **1a** but using the cyclohexyl-substituted phosphonium dimer (321 mg, 0.5 mmol). Pale-yellow oil that was used without further purification (136 mg, 43%). ^{31}P{^{1}H} NMR (242 MHz, $CDCl_3$) δ: -10.57 ppm. ^{1}H (500 MHz, $CDCl_3$) δ: 1.16-1.24, m(br), 10H, (Cy-CH_2), 1.52-1.57, m(br), 2H, (Cy-CH), 1.66-1.78, m(br), 12H, (Cy-CH_2 & P-CH_2), 3.35-3.40, q(br), 2H (P-CH_2), 4.90, s(br), 1H (NH), 6.36, d(br), 1H, (py-H), 6.52-6.55, m, 1H, (py-H), 7.36-7.40, m, 1H, (py-H), 8.07, s(br), 1H, (py-H). MS-DART m/z calculated for $[C_{19}H_{31}N_2P]^+$: 319.2298, found: 319.2304.

***N*-(2-(diisobutylphosphinyl)ethyl)pyridin-2-amine (1c)**

The same general procedure was followed as in the synthesis of **1a** but using the *iso*butyl-substituted phosphonium dimer (269 mg, 0.5 mmol). Colourless oil that was used without further purification (106 mg, 40%). ^{31}P{^{1}H} NMR (242 MHz, $CDCl_3$) δ: -44.19 ppm. ^{1}H (600 MHz, $CDCl_3$) δ: 0.96, d (*J* = 3.2 Hz), 6H, (^{i}Bu-CH_3), 0.97, d (*J* = 3.2 Hz), 6H, (^{i}Bu-CH_3), 1.28-1.36, m, 4H, (^{i}Bu-CH_2), 1.65-1.70, m, 4H, (^{i}Bu-C*H* & CH_2), 3.35-3.40, m, 2H, (CH_2), 4.68, s(br), 1H, (N*H*), 6.34-6.35, dd (*J* = 8.4, 1.0 Hz), 1H, (py-*H*), 6.51-6.53, m, 1H, (py-*H*), 7.35-7.38, m, 1H, (py-*H*), 8.05-8.06, m, 1H, (py-*H*). MS-DART m/z calculated for $[C_{15}H_{27}N_2P]^+$: 267.1985, found: 267.1992.

***N*-(2-(diphenylphosphinyl)ethyl)quinolin-8-amine (2a)**

A vial was charged with 8-aminoquinoline (144 mg, 1.0 mmol), the phenyl-substituted phosphonium dimer (309 mg, 0.5 mmol), and sodium(triacetoxy)borohydride (424 mg, 2.0 mmol). 3 Å molecular sieves were added. THF (8 mL) was added and the blood-red mixture was stirred for 18 h at room temperature. The solvent was evaporated under vacuum and the residue was dissolved in DCM (10 mL). An air-free wash of the organic layer with saturated NH_4Cl (2x 10 mL) and water (2x 10 mL) was carried out. The organic layer was dried over Na_2SO_4, filtered and dried under vacuum to give an orange-red oil that was used without further purification (191 mg, 54%). ^{31}P{^{1}H} NMR (202 MHz, $CDCl_3$) δ: -21.09 ppm. ^{1}H NMR (500 MHz, $CDCl_3$) δ: 2.55-2.59, m, 2H, (CH_2), 3.48-3.53, m, 2H, (CH_2), 6.33, s(br), 1H, (N*H*), 6.54-6.56, dd (*J* = 7.7, 1.1 Hz), 1H, (Ar-*H*), 7.04-7.06, dd (*J* = 8.2, 1.2 Hz), 1H, (Ar-*H*), 7.33-7.52, m, 12H, (Ar-*H*, P*Ph*$_2$), 8.04-8.05, dd (*J* = 8.2, 1.7 Hz), 1H, (Ar-*H*), 8.71-8.72, dd (*J* = 4.2, 1.7 Hz), 1H, (Ar-*H*). ^{13}C NMR (126 MHz, $CDCl_3$) δ: 28.39, d, (*J* = 13.2 Hz) (CH_2), 40.47, d, (*J* = 23.7 Hz) (CH_2), 104.73, 114.02, 121.45, 127.80 (*Ar–C*), 128.63, d, ($^3J_{CP}$ = 6.8 Hz) (*P–PhCH*), 128.74 (*P–Ph; paraCH)*, 128.84 (*Ar–C*), 132.87, d, ($^2J_{CP}$ = 18.7 Hz) (*P–PhCH*), 136.03 (*Ar–C*), 138.18, d, ($^1J_{CP}$ = 12.3 Hz) (*P–PhC*), 138.32, 144.33, 146.92 (*Ar–C*). MS-DART m/z calculated for $[C_{23}H_{21}N_2P]^+$: 357.1515, found: 357.1525.

***N*-(2-(dicyclohexylphosphinyl)ethyl)quinolin-8-amine (2b)**

The same general procedure was followed as in the synthesis of **2a** but using the cyclohexyl-substituted phosphonium dimer (321 mg, 0.5 mmol). Orange-red oil that was used without further purification (209 mg, 57%). ^{31}P{^{1}H} NMR (202 MHz, CDCl3) δ: -8.61 ppm. ^{1}H NMR (500 MHz, CDCl3) δ: 1.17-1.30, m(br), 10H, (Cy-CH_2), 1.57-1.62, m(br), 2H, (Cy-CH) (Cy 1.69-1.79, m(br), 10H, (Cy), 1.85-1.89, m, 2H, (CH_2), 3.41-3.46, m, 2H, (CH_2), 6.30, s(br), 1H, (NH), 6.66-6.67, dd (J = 7.7, 1.1 Hz), 1H, (Ar-H), 7.02-7.05, m, 1H, (Ar-H), 7.34-7.40, m, 2H, (Ar-H), 8.03-8.05, dd (J = 8.3, 1.7 Hz), 1H, (Ar-H), 8.70-8.71, dd (J = 4.2, 1.7 Hz), 1H, (Ar-H). ^{13}C NMR (126 MHz, CDCl3) δ: 21.83, d, (J = 17.7 Hz) (P-CH2), 27.36, d, (J = 7.5 Hz) (Cy-CH2), 27.46, d, (J = 11.6 Hz) (Cy-CH2), 29.07, d, (J = 7.7 Hz) (Cy-CH2), 30.41, d, (J = 14.5 Hz) (Cy-CH2), 33.37, d, (J = 11.6 Hz) (Cy-CH), 43.23, d, (J = 30.8 Hz) (P-CH2), Ar–C: 104.84, 113.88, 121.46, 127.92, 128.79, 136.08, 138.31, 144.58, 146.92. MS-DART m/z calculated for $[C_{25}H_{33}N_2P]^+$: 369.2454, found: 369.2459.

***N*-(2-(diisobutylphosphinyl)ethyl)quinolin-8-amine (2c)**

The same general procedure was followed as in the synthesis of **2a** but using the *iso*butyl-substituted -phosphonium dimer (269 mg, 0.5 mmol). Orange-red oil that was used without further purification (187 mg, 59%). ^{31}P{^{1}H} NMR (202 MHz, $CDCl_3$) δ: -42.60 ppm. ^{1}H NMR (500 MHz, $CDCl_3$) δ: 1.02, d (*J* = 4.0 Hz), 6H, (^{i}Bu-CH_3), 1.03, d (*J* = 4.0 Hz), 6H, (^{i}Bu-CH_3), 1.35-1.45, m, 4H, (^{i}Bu-CH_2), 1.70-1.80, m, 2H, (^{i}Bu-C*H*), 1.85-1.89, m, 2H, (CH_2), 3.44-3.48, m, 2H, (CH_2), 6.23, s(br), 1H, (N*H*), 6.66-6.68, m, 1H, (Ar-*H*), 7.03-7.06, m, 1H, (Ar-*H*), 7.34-7.41, m, 2H, (Ar-*H*), 8.03-8.05, dd (*J* = 8.2, 1.7 Hz), 1H, (Ar-*H*), 8.71-8.72, dd (*J* = 4.2, 1.7

View Article Online DOI: 10.1039/C8DT04058C

Hz), 1H, (Ar-*H*). ^{13}C NMR (126 MHz, $CDCl_3$) δ: 24.42, d, (*J* = 9.2 Hz) (*CH*$_3$), 24.52, d, (*J* = 9.0 Hz) (*CH*$_3$), 26.68, d, (*J* = 13.3 Hz) (*CH*), 29.06, d, (*J* = 14.2 Hz) (*CH*$_2$), 39.35, d, (*J* = 12.7 Hz) (i-Bu *CH*$_2$), 40.98, d, (*J* = 20.5 Hz) (*CH*$_2$), Ar-C: 104.72, 113.91, 121.47, 127.88, 128.72, 136.06, 138.33, 144.62, 146.92. MS-DART m/z calculated for $[C_{19}H_{29}N_2P]^+$: 317.2141, found: 317.2144.

***N*-(2-(diisopropylphosphinyl)ethyl)quinolin-8-amine (2d)**

The same general procedure was followed as in the synthesis of **2a** but using isopropyl-substituted phosphonium dimer (241 mg, 0.5 mmol). Orange-red oil that was used without further purification (164 mg, 57%). $^{31}P\{^1H\}$ NMR (202 MHz, CDCl3) δ: -0.33 ppm. ^{1}H NMR (500 MHz, CDCl3) δ: 1.09-1.15, m, 12H, (iPr-CH3), 1.78-1.82, qd (J = 7.1, 2.4 Hz), 2H, (CH), 1.83-1.87, m, 2H, (CH2) 3.45-3.50, m, 2H, (CH2), 6.28, s(br), 1H, (NH), 6.66-6.68, m, 1H, (Ar-H), 7.03-7.05, m, 1H, (Ar-H), 7.34-7.40, m, 2H, (Ar-H), 8.04-8.06, dd (J = 8.3, 1.7 Hz), 1H, (Ar-H), 8.71-8.71, dd (J = 4.2, 1.6 Hz), 1H, (Ar-H). ^{13}C NMR (126 MHz, CDCl3) δ: 18.85, d, (J = 9.0 Hz) (CH3), 20.21, d, (J = 16.0 Hz) (CH3), 22.00, d, (J = 18.3 Hz) (CH2), 23.47, d, (J = 11.3 Hz) (CH), 42.98, d, (J = 29.7 Hz) (CH2), Ar–C: 104.82, 113.93, 121.47, 127.92, 128.80, 136.08, 138.34, 144.57, 146.95. MS-DART m/z calculated for $[C_{17}H_{25}N_2P]^+$: 289.1828, found: 289.1830.

2-(diphenylphosphinyl)-*N*-(2-(diphenylphosphaneyl)ethyl)-*N*-(pyridin-2-ylmethyl)ethan-1-amine (3a)

A vial was charged with 2-picolylamine (54 mg, 0.5 mmol), phenyl-substituted phosphonium dimer (309 mg, 0.5 mmol), and sodium(triacetoxy)borohydride (424 mg, 2.0 mmol). 3 Å molecular sieves were added. THF (6 mL) was added and the mixture was stirred for 18 h at room temperature. The solvent was evaporated under reduced pressure and the residue was dissolved in DCM (10 mL). An air-free wash of the organic layer with saturated NH_4Cl (2x 10 mL) and water (2x 10 mL) was carried out. The organic layer was dried over Na_2SO_4, filtered and was dried under vacuum to give a viscous yellow oil that solidified on standing that was used without further purification (161 mg, 61%). $^{31}P\{^1H\}$ NMR (202 MHz, $CDCl_3$) δ: -20.16 ppm. ^{1}H NMR (500 MHz, $CDCl_3$) δ: 2.15, s(br), 4H, (*CH*$_2$), 2.64, s(br), 4H, (*CH*$_2$), 3.75, s(br), 2H, (picolyl-*CH*$_2$), 7.10, s(br), 1H, (Py-*H*), 7.27-7.36, m, 22H, (P*Ph*$_2$, Py-*H*), 8.45-8.47, m, 1H, (Py-*H*). MS-DART m/z calculated for $[C_{34}H_{34}N_2P_2]^+$: 533.2270, found: 533.2279.

2-(dicyclohexylphosphinyl)-*N*-(2-(dicyclohexylphosphaneyl)ethyl)-*N*-(pyridin-2-ylmethyl)ethan-1-amine (3b)

The same general procedure was followed as in the synthesis of **3a** but with Cy-phosphonium dimer (321 mg, 0.5 mmol). The filtrate was passed through a short neutral alumina plug. Colourless oil (105 mg, 38%). $^{31}P\{^1H\}$ NMR (202 MHz, $CDCl_3$) δ: -7.79 ppm. ^{1}H NMR (500 MHz, $CDCl_3$) δ: 1.07-1.24, m, 20H, (P*Cy*$_2$), 1.45-1.50, m, 4H, (Cy-C*H*), 1.54-1.58, m, 4H, (*CH*$_2$), 1.64-1.75, m, 20H, (P*Cy*$_2$), 2.63-2.67, m, 4H, (*CH*$_2$), 3.77, s, 2H, (picolyl-*CH*$_2$), 7.11-7.13, m, 1H, (Py-*H*), 7.45-7.46, d (*J* = 7.8 Hz), 1H, (Py-*H*), 7.60-7.63, td (*J* = 7.7, 1.9 Hz), 1H, (Py-*H*), 8.51-8.52, m, 1H, (Py-*H*). MS-DART m/z calculated for $[C_{34}H_{58}N_2P_2]^+$: 557.4148, found: 557.4151.

2-(diisobutylphosphinyl)-N-(2-(diisobutylphosphaneyl)ethyl)-N-(pyridin-2-ylmethyl)ethan-1-amine (3c)

The same general procedure was followed as in the synthesis of **3a** but with the *iso*butyl-substituted -phosphonium dimer (269 mg, 0.5 mmol). The filtrate was passed through a short neutral alumina plug. Colourless oil (73 mg, 32%). $^{31}P\{^1H\}$ NMR (202 MHz, $CDCl_3$) δ: -42.00 ppm. ^{1}H NMR (500 MHz, $CDCl_3$) δ: 0.93-0.95, m, 24H, (^{i}Bu-C*H*$_3$), 1.20-1.29, m, 8H, (^{i}Bu-C*H*$_2$), 1.52-1.54, m, 4H, (*CH*$_2$), 1.57-1.67, m, 4H, (^{i}Bu-C*H*), 2.61-2.65, m, 4H, (*CH*$_2$), 3.73, s, 2H, (picolyl-*CH*$_2$), 7.10-7.12, ddd (*J* = 7.5, 4.9, 1.8 Hz), 1H, (Py-*H*), 7.45-7.46, m, 1H, (Py-*H*), 7.59-7.62, td (*J* = 7.6, 1.8 Hz), 1H, (Py-*H*), 8.49-8.50, ddd (*J* = 4.9, 1.9, 0.9 Hz), 1H, (Py-*H*). MS-DART m/z calculated for $[C_{26}H_{50}N_2P_2]^+$: 453.3522, found: 453.3526.

Co_2Cl_4(APyPNN-Cy)$_2$ (4)

A vial was charged with $CoCl_2$ (50 mg, 0.38 mmol) and THF (6 mL) and stirred for 30 min. **1a** (136 mg, 0.43 mmol) was dissolved in THF (2 mL) and added dropwise. The solution immediately darkened to a navy-blue colour. Stirring was continued overnight. The solvent volume was reduced to ~1 mL under reduced pressure and then 4 mL of pentane was added to the rapidly stirring solution to which a blue-green solid precipitated out. The solid was collected via filtration, washed with pentane (4 mL), and dried under vacuum to give a blue-green solid (100 mg, 30%). Crystals suitable for X-ray diffraction were grown by layering Et_2O on top of a saturated toluene solution. μ_{eff} (Evans Method) = 5.4 ± 0.2. Anal. Calcd for $C_{38}H_{62}Cl_4Co_2N_4P_2$: C, 50.91; H, 6.97; N, 6.25. Found: C, 50.15; H, 7.16; N, 4.71*. *EA was attempted three times and a low nitrogen content was observed in all cases.

Co_2Cl_4(APyPNN-iBu)$_2$ (5)

A vial was charged with $CoCl_2$ (25 mg, 0.19 mmol) and THF (6 mL) and stirred for 30 min. **1b** (57 mg, 0.21 mmol) was dissolved in THF (1 mL) and added dropwise. An immediate darkening of the solution was observed and stirring continued overnight. The solution was concentrated to dryness and the residue re-dissolved in THF (3 mL). The solution was added to a rapidly stirring vial containing pentane (10 mL) and a navy blue solid precipitated, stirring continued overnight. The solid was isolated by filtration and dried under vacuum to give a navy blue solid powder (60 mg, 40%). Crystals suitable for X-ray diffraction were grown via slow evaporation of a toluene/DCM/THF solution. μ_{eff} (Evans Method) = 5.8 ± 0.3. Anal. calcd for $C_{30}H_{54}Cl_4Co_2N_4P_2$: C, 45.47; H, 6.87; N, 7.07. Found: C, 45.71; H, 6.88; N, 6.77.

$CoCl_2$(AQPNN-Ph) (6)

A vial was charged with $CoCl_2$ (54 mg, 0.42 mmol) and THF (6 mL) and stirred for 30 min. **2a** (150 mg, 0.42 mmol) was dissolved in THF (2 mL) and added dropwise to which an immediate colour change to dark blue-green occurred and then to purple upon complete addition of the ligand. The mixture

View Article Online
DOI: 10.1039/C8DT04058C

was stirred overnight and the appearance of a precipitate was observed. The mixture was filtered and the solid was collected on a frit, washed with pentane (8 mL), and dried under vacuum to give a magenta coloured solid (186 mg, 91%). Crystals suitable for X-ray diffraction were grown via slow diffusion of pentane into a saturated DCM solution. τ_5 = 0.75. μ_{eff} (Evans Method) = 3.9 ± 0.1. Anal. calcd for $C_{23}H_{21}Cl_2CoN_2P$: C, 56.81; H, 4.35; N, 5.76. Found: C, 56.75; H, 4.59; N, 5.31.

$CoCl_2$(AQPNN-Cy) (7)

A vial was charged with $CoCl_2$ (55 mg, 0.43 mmol) and THF (6 mL) and stirred for 30 min. **2b** (175 mg, 0.48 mmol) was dissolved in THF (2 mL) and added dropwise to which an immediate colour change to magenta occurred. The mixture was stirred for an additional 1 h and then the solvent volume was reduced to ~1 mL under vacuum. 6 mL of pentane was added to the rapidly stirring solution and a magenta solid precipitated out. The solid was collected via filtration and washed with pentane (5 mL), Et2O (2 mL), and dried under vacuum to yield a magenta coloured solid (172 mg, 81%). Crystals suitable for X-ray diffraction were grown via slow diffusion of pentane into a saturated DCM solution. τ_5 = 0.90. μ_{eff} (Evans Method) = 4.2 ± 0.1. Anal. calcd for $C_{23}H_{33}Cl_2CoN_2P$: C, 55.43; H, 6.67; N, 5.62. Found: C, 55.67; H, 6.65; N, 5.34.

$CoCl_2$(AQPNN-^{i}Bu) (8)

A vial was charged with $CoCl_2$ (59 mg, 0.46 mmol) and THF (6 mL) and stirred for 30 min. **2d** (148 mg, 0.46 mmol) was dissolved in THF (2 mL) and added dropwise to which an immediate colour change to dark blue-green occurred and then to magenta upon complete addition of the ligand. The mixture was stirred overnight and the appearance of a precipitate was observed. The mixture was filtered and the solid was collected on a frit, washed with pentane (8 mL), and dried under vacuum to give a fluffy magenta coloured solid (154 mg, 75%). Crystals suitable for X-ray diffraction were grown via slow diffusion of pentane into a saturated DCM solution. τ_5 = 0.67. μ_{eff} (Evans Method) = 4.2 ± 0.3. Anal. calcd for $C_{19}H_{29}Cl_2CoN_2P$: C, 51.14; H, 6.55; N, 6.28. Found: C, 50.85; H, 6.56; N, 6.12.

$FeCl_2$(AQPNN-^{i}Pr) (9)

A vial was charged with $FeCl_2$ (59 mg, 0.47 mmol) and THF (8 mL). **2c** (136 mg, 0.47 mmol) was dissolved in THF (2 mL) and added dropwise. An immediate colour change to blood-red was observed along with the precipitation of a solid. The mixture was stirred overnight and then the solvent volume was reduced to ~1 mL under reduced pressure. 8 mL of pentane was added to the rapidly stirring solution. The product was collected via filtration and dried under vacuum to give a blood-red solid powder (169 mg, 87%). Crystals suitable for XRD were grown by slow diffusion of pentane into a saturated DCM solution. τ_5 = 0.81. μ_{eff} (Evans Method) = 3.9 ± 0.3. μ_{eff} (solid) = 5.2. Anal. Calcd for $C_{17}H_{25}Cl_2FeN_2P$: C, 49.19; H, 6.07; N, 6.75. Found: C, 49.25; H, 5.93; N, 6.53.

$[FeCl_2$(AQPNN-Ph)$]_2$ (10)

A vial was charged with $FeCl_2$ (80 mg, 0.63 mmol) and THF (8 mL) and stirred for 2 h. **2a** (225 mg, 0.63 mmol) was dissolved in THF (2 mL) and added dropwise. An immediate colour change to red was observed along with precipitation of a solid. The mixture was stirred overnight and then the solvent volume was reduced to ~1 mL under reduced pressure. 8 mL of pentane was added to the rapidly stirring solution. The product was collected via filtration and dried under vacuum to give a red powder (276 mg, 91%). Crystals suitable for XRD were grown by slow diffusion of pentane into a DCM solution. μ_{eff} (solid) = 7.4. Anal. Calcd for $C_{46}H_{42}Cl_4Fe_2N_4P_2$: C, 57.18; H, 4.38; N, 5.80. Found: C, 57.33; H, 4.84; N, 5.27.

$FeCl_2$(P_2NN') (11)

A vial was charged with $FeCl_2$ (23 mg, 0.18 mmol) and THF (10 mL). Fe powder was added (120 mg) and the mixture was stirred overnight. The mixture was filtered over a pad of celite to give a colourless solution of $FeCl_2$ in THF. **3a** (98 mg, 0.18 mmol) was dissolved in THF (1 mL) and added dropwise. An immediate colour change to yellow was observed and then orange upon full addition of the ligand. After ~2 h of continued stirring a yellow solid precipitated out of solution. Stirring continued overnight and then the precipitate was collected by filtration to give a yellow solid (100 mg, 83%). Crystals suitable for X-ray diffraction were grown by slow diffusion of pentane into a saturated DCM solution. μ_{eff} (Evans Method) = 4.7 ± 0.3. Anal. Calcd for $C_{34}H_{34}Cl_2FeN_2P_2$: C, 61.94; H, 5.20; N, 4.25. Found: C, 59.77*; H, 5.07; N, 4.21. *EA was attempted three times and a low carbon weight was observed in all cases.

Acknowledgements

R. H. Morris thanks NSERC for a Discovery Grant and a Strategic Grant "Catalytic Synthesis of Specialty Chemicals from Sustainable Resources". The authors wish to acknowledge the Canadian Foundation for Innovation, project number 19119, and the Ontario Research Fund for funding of the Centre for Spectroscopic Investigation of Complex Organic Molecules and Polymers. Dr. P. A. Dube of the Brockhouse Institute for Materials Research at McMaster University is acknowledged for solid state magnetic susceptibility measurements.

References

1 J. Yuwen, S. Chakraborty, W. W. Brennessel and W. D. Jones, *ACS Catal.*, 2017, **7**, 3735–3740.
2 G. Zhang, J. Wu, H. Zeng, S. Zhang, Z. Yin and S. Zheng, *Org. Lett.*, 2017, **19**, 1080–1083.
3 S. Kuriyama, K. Arashiba, H. Tanaka, Y. Matsuo, K. Nakajima, K. Yoshizawa and Y. Nishibayashi, *Angew. Chem. Int. Ed.*, 2016, **55**, 14291–14295.
4 G. Zhang, B. L. Scott and S. K. Hanson, *Angew. Chem. Int. Ed.*, 2012, **51**, 12102–12106.
5 V. M. Krishnan, H. D. Arman and Z. J. Tonzetich, *Dalton Trans.*, 2018, **47**, 1435–1441.

6 A. Z. Spentzos, C. L. Barnes and W. H. Bernskoetter, *Inorg. Chem.*, 2016, **55**, 8225–8233.
7 M. Andérez-Fernández, L. K. Vogt, S. Fischer, W. Zhou, H. Jiao, M. Garbe, S. Elangovan, K. Junge, H. Junge, R. Ludwig and M. Beller, *Angew. Chem. Int. Ed.*, 2017, **56**, 559–562.
8 N. V. Kulkarni, W. W. Brennessel and W. D. Jones, *ACS Catal.*, 2017, 997–1002.
9 S. Elangovan, M. Garbe, H. Jiao, A. Spannenberg, K. Junge and M. Beller, *Angew. Chem. Int. Ed.*, 2016, **55**, 15364–15368.
10 D. H. Nguyen, X. Trivelli, F. Capet, J.-F. Paul, F. Dumeignil and R. M. Gauvin, *ACS Catal.*, 2017, **7**, 2022–2032.
11 M. Peña-López, P. Piehl, S. Elangovan, H. Neumann and M. Beller, *Angew. Chem. Int. Ed.*, 2016, **55**, 14967–14971.
12 S. Chakraborty, U. Gellrich, Y. Diskin-Posner, G. Leitus, L. Avram and D. Milstein, *Angew. Chem. Int. Ed.*, 2017, **56**, 4229–4233.
13 S. Fu, Z. Shao, Y. Wang and Q. Liu, *J. Am. Chem. Soc.*, 2017, **139**, 11941–11948.
14 M. Garbe, K. Junge, S. Walker, Z. Wei, H. Jiao, A. Spannenberg, S. Bachmann, M. Scalone and M. Beller, *Angew. Chem. Int. Ed.*, 2017, **56**, 11237-11241.
15 M. Mastalir, B. Stöger, E. Pittenauer, M. Puchberger, G. Allmaier and K. Kirchner, *Adv. Synth. Catal.*, 2016, **358**, 3824–3831.
16 N. T. Fairweather, M. S. Gibson and H. Guan, *Organometallics*, 2015, **34**, 335–339.
17 S. Werkmeister, K. Junge, B. Wendt, E. Alberico, H. Jiao, W. Baumann, H. Junge, F. Gallou and M. Beller, *Angew. Chem. Int. Ed.*, 2014, **53**, 8722–8726.
18 S. Elangovan, B. Wendt, C. Topf, S. Bachmann, M. Scalone, A. Spannenberg, H. Jiao, W. Baumann, K. Junge and M. Beller, *Adv. Synth. Catal.*, 2016, **358**, 820–825.
19 S. Chakraborty, H. Dai, P. Bhattacharya, N. T. Fairweather, M. S. Gibson, J. A. Krause and H. Guan, *J. Am. Chem. Soc.*, 2014, **136**, 7869–7872.
20 I. Koehne, T. J. Schmeier, E. A. Bielinski, C. J. Pan, P. O. Lagaditis, W. H. Bernskoetter, M. K. Takase, C. Würtele, N. Hazari and S. Schneider, *Inorg. Chem.*, 2014, **53**, 2133–2143.
21 T. Zell, Y. Ben-David and D. Milstein, *Angew. Chem. Int. Ed.*, 2014, **53**, 4685–4689.
22 S. Chakraborty, G. Leitus and D. Milstein, *Angew. Chem. Int. Ed.*, 2017, **56**, 2074–2078.
23 F. Schneck, M. Assmann, M. Balmer, K. Harms and R. Langer, *Organometallics*, 2016, **35**, 1931–1943.
24 P. O. Lagaditis, P. E. Sues, J. F. Sonnenberg, K. Y. Wan, A. J. Lough and R. H. Morris, *J. Am. Chem. Soc.*, 2014, **136**, 1367–1380.
25 S. A. M. Smith, P. O. Lagaditis, A. Lüpke, A. J. Lough and R. H. Morris, *Chem. Eur. J.*, 2017, **23**, 7212–7216.
26 M. Peña-López, H. Neumann and M. Beller, *ChemCatChem*, 2015, **7**, 865–871.
27 E. A. Bielinski, P. O. Lagaditis, Y. Zhang, B. Q. Mercado, C. Würtele, W. H. Bernskoetter, N. Hazari and S. Schneider, *J. Am. Chem. Soc.*, 2014, **136**, 10234–10237.
28 S. Chakraborty, P. O. Lagaditis, M. Förster, E. A. Bielinski, N. Hazari, M. C. Holthausen, W. D. Jones and S. Schneider, *ACS Catal.*, 2014, **4**, 3994–4003.
29 Y. Zhang, A. D. MacIntosh, J. L. Wong, E. A. Bielinski, P. G. Williard, B. Q. Mercado, N. Hazari and W. H. Bernskoetter, *Chem. Sci.*, 2015, **6**, 4291–4299.
30 J. F. Sonnenberg, A. J. Lough and R. H. Morris, *Organometallics*, 2014, **33**, 6452–6465.
31 S. W. Kohl, L. Weiner, L. Schwartsburd, L. Konstantinovski, L. J. W. Shimon, Y. Ben-David, M. A. Iron and D. Milstein, *Science*, 2009, **324**, 74–77.
32 D. Vuzman, E. Poverenov, L. J. W. Shimon, Y. Diskin-Posner and D. Milstein, *Organometallics*, 2008, **27**, 2627–2634.
33 M. H. G. Prechtl, K. Wobser, N. Theyssen, Y. Ben-David, D. Milstein and W. Leitner, *Cat. Sci. Technol.*, 2012, **2**, 2039–2042.
34 E. Balaraman, D. Srimani, Y. Diskin-Posner and D. Milstein, *Catal Lett*, 2015, **145**, 139–144.
35 J. Zhang, M. Gandelman, L. J. W. Shimon and D. Milstein, *Dalton Trans.*, 2006, **0**, 107–113.
36 J. Zhang, G. Leitus, Y. Ben-David and D. Milstein, *J. Am. Chem. Soc.*, 2005, **127**, 10840–10841.
37 D. Srimani, E. Balaraman, P. Hu, Y. Ben-David and D. Milstein, *Adv. Synth. Catal.*, 2013, **355**, 2525–2530.
38 W. Li, J.-H. Xie, H. Lin and Q.-L. Zhou, *Green Chem.*, 2012, **14**, 2388–2390.
39 L. Zhang, Z. Han, X. Zhao, Z. Wang and K. Ding, *Angew. Chem. Int. Ed.*, 2015, **54**, 6186–6189.
40 E. Fogler, M. A. Iron, J. Zhang, Y. Ben-David, Y. Diskin−Posner, G. Leitus, L. J. W. Shimon and D. Milstein, *Inorg. Chem.*, 2013, **52**, 11469–11479.
41 E. Kinoshita, K. Arashiba, S. Kuriyama, A. Eizawa, K. Nakajima and Y. Nishibayashi, *Eur. J. Inorg. Chem.*, 2015, **2015**, 1789–1794.
42 K. Arashiba, K. Nakajima and Y. Nishibayashi, *Z. anorg. allg. Chem.*, 2015, **641**, 100–104.
43 A. V. Polezhaev, C. J. Liss, J. Telser, C.-H. Chen and K. G. Caulton, *Chem. Eur. J.*, 2018, **24**, 1330–1341.
44 D. Srimani, A. Mukherjee, A. F. G. Goldberg, G. Leitus, Y. Diskin-Posner, L. J. W. Shimon, Y. Ben David and D. Milstein, *Angew. Chem. Int. Ed.*, 2015, **54**, 12357–12360.
45 T. Zell, P. Milko, K. L. Fillman, Y. Diskin-Posner, T. Bendikov, M. A. Iron, G. Leitus, Y. Ben-David, M. L. Neidig and D. Milstein, *Chem. Eur. J.*, 2014, **20**, 4403–4413.
46 N. A. Espinosa-Jalapa, A. Kumar, G. Leitus, Y. Diskin-Posner and D. Milstein, *J. Am. Chem. Soc.*, 2017, **139**, 11722–11725.
47 T. Zell, R. Langer, M. A. Iron, L. Konstantinovski, L. J. W. Shimon, Y. Diskin-Posner, G. Leitus, E. Balaraman, Y. Ben-David and D. Milstein, *Inorg. Chem.*, 2013, **52**, 9636–9649.
48 A. V. Polezhaev, C.-H. Chen, Y. Losovyj and K. G. Caulton, *Chem. Eur. J.*, 2017, **23**, 8039–8050.
49 S. Samanta, S. Demesko, S. Dechert and F. Meyer, *Angew. Chem. Int. Ed.*, 2015, **54**, 583–587.
50 D. Peng, Y. Zhang, X. Du, L. Zhang, X. Leng, M. D. Walter and Z. Huang, *J. Am. Chem. Soc.*, 2013, **135**, 19154–19166.
51 Z. Shao, S. Fu, M. Wei, S. Zhou and Q. Liu, *Angew. Chem. Int. Ed.*, 2016, **55**, 14653–14657.
52 S. A. M. Smith and R. H. Morris, *Synthesis*, 2015, **47**, 1775–1779.
53 S. A. M. Smith, D. E. Prokopchuk and R. H. Morris, *Isr. J. Chem.*, 2017, **57**, 1204–1215.
54 A. A. Mikhailine and R. H. Morris, *Inorg. Chem.*, 2010, **49**, 11039–11044.
55 A. Mikhailine, A. J. Lough and R. H. Morris, *J. Am. Chem. Soc.*, 2009, **131**, 1394–1395.
56 K. Z. Demmans, C. S. G. Seo, A. J. Lough and R. H. Morris, *Chem. Sci.*, 2017, **8**, 6531–6541.
57 W. Zuo, S. Tauer, D. E. Prokopchuk and R. H. Morris, *Organometallics*, 2014, **33**, 5791–5801.
58 J. F. Sonnenberg, K. Y. Wan, P. E. Sues and R. H. Morris, *ACS Catal.*, 2017, **7**, 316–326.
59 P. E. Sues, A. J. Lough and R. H. Morris, *Organometallics*, 2011, **30**, 4418–4431.
60 A. A. Mikhailine, E. Kim, C. Dingels, A. J. Lough and R. H. Morris, *Inorg. Chem.*, 2008, **47**, 6587–6589.

View Article Online
DOI: 10.1039/C8DT04058C

61 P. O. Lagaditis, A. A. Mikhailine, A. J. Lough and R. H. Morris, *Inorg. Chem.*, 2010, **49**, 1094–1102.
62 W. Zuo, A. J. Lough, Y. F. Li and R. H. Morris, *Science*, 2013, **342**, 1080–1083.
63 A. A. Mikhailine, P. O. Lagaditis, P. E. Sues, A. J. Lough and R. H. Morris, *J. Organomet. Chem.*, 2010, **695**, 1824–1830.
64 E. Peris and R. H. Crabtree, *Chem. Soc. Rev.*, 2018, **47**, 1959–1968.
65 A. F. Abdel-Magid and S. J. Mehrman, *Org. Process Res. Dev.*, 2006, **10**, 971–1031.
66 Y.-J. Tsai, U. H. Lee and Q. Zhao, *Polyhedron*, 2017, **124**, 206–214.
67 S. Jie, M. Agostinho, A. Kermagoret, C. S. J. Cazin and P. Braunstein, *Dalton Trans.*, 2007, **0**, 4472–4482.
68 L.-C. Liang, P.-S. Chien and P.-Y. Lee, *Organometallics*, 2008, **27**, 3082–3093.
69 X. Liu, W. Zhang, Y. Wang, Z.-X. Zhang, L. Jiao and Q. Liu, *J. Am. Chem. Soc.*, 2018, **140**, 6873–6882.
70 A. W. Addison, T. N. Rao, J. Reedijk, J. van Rijn and G. C. Verschoor, *J. Chem. Soc., Dalton Trans.*, 1984, **0**, 1349–1356.
71 M. U. Anwar, K. V. Shuvaev, L. N. Dawe and L. K. Thompson, *Inorg. Chem.*, 2011, **50**, 12141–12154.
72 C. J. Davies, G. A. Solan and J. Fawcett, *Polyhedron*, 2004, **23**, 3105–3114.
73 C. Holzhacker, M. J. Calhorda, A. Gil, M. D. Carvalho, L. P. Ferreira, B. Stöger, K. Mereiter, M. Weil, D. Müller, P. Weinberger, E. Pittenauer, G. Allmaier and K. Kirchner, *Dalton Trans.*, 2014, **43**, 11152–11164.

View Article Online
DOI: 10.1039/C8DT04058C

TOC entry

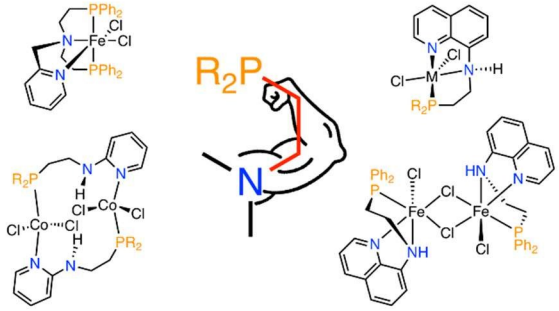

Phosphorus-donor “arms” are readily added to amines in order to enable sturdy base metal coordination.